

Mechanism of the Palladium-Catalyzed Borylation of Aryl Halides with Pinacolborane

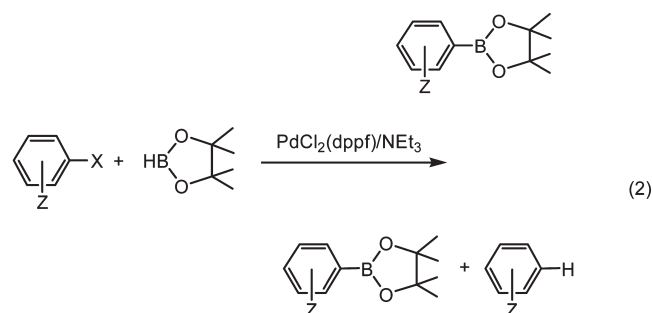
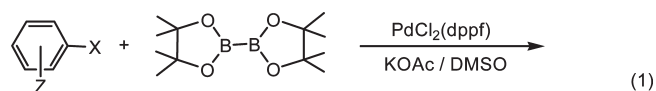
King Chung Lam,[†] Todd B. Marder,^{*,‡} and Zheyang Lin^{*,†}[†]Department of Chemistry, Hong Kong University of Science and Technology, Clear Water Bay, Kowloon, Hong Kong, and [‡]Department of Chemistry, Durham University, South Road, Durham, DH1 3LE, U.K.

Received December 17, 2009

With the aid of DFT calculations, we have examined the mechanism of the widely employed Pd-catalyzed borylation of aryl halides using HBpin (pin = OCMe₂CMe₂O) developed by Masuda et al. In contrast to their original proposed mechanism involving an ammonium boride ion pair in the transmetalation step that follows aryl halide oxidative addition to Pd(0), our calculations support a transmetalation process that involves σ -bond metathesis between HBpin and a cationic [L₂Pd(Ar)]⁺ species as the ArBpin product generating step. The new mechanism is also applicable to the related boration reaction employing R₂NBH₂ reagents developed by Alcaraz et al.

Introduction

Arylboronic acids and their esters are versatile and useful reagents in organic synthesis.¹ Traditionally, arylboron compounds are prepared by transmetalation between aryl-magnesium or aryllithium reagents and trialkylborates.^{1g,2,3} While the recently developed rhodium- and iridium-catalyzed direct borylation of arene C–H bonds represents a major breakthrough,⁴ the palladium-catalyzed cross-coupling⁵ of bis(pinacolato)diborane(4) (B₂pin₂) (pin = pinacolato = OCMe₂CMe₂O) with aryl halides (eq 1), reported by Miyaura et al. in 1995, still represents one of the most important synthetic routes to arylboronates.⁶ The cost of B₂pin₂, however, led Masuda et al. to develop an attractive, alternative palladium-catalyzed process using HBpin (eq 2).⁷ Although the price of B₂pin₂ and B₂(neop)₂ (neop = neopentylglycolato = OCH₂CMe₂CH₂O) has dropped significantly since then and both are now available in > 50 kg quantities, and alternative nickel-⁸ and copper-catalyzed⁹ ArX borylation processes have been developed, Masuda's route is also still widely employed.



On the basis of their experimental findings, Masuda et al. proposed a mechanism (Scheme 1) to account for the palladium-catalyzed ArX + HBpin cross-coupling reaction. In the proposed mechanism, an oxidative addition of the aryl halide to a palladium(0) complex, which affords a stable *trans*-palladium(II) complex Ar-Pd^{II}-X, was considered as the first step. Then, the halide ligand is replaced by a boryl group in a transmetalation step. Subsequently, a reductive elimination of the arylboronate Ar-B(OR)₂ takes place, along with regeneration of the catalyst.

In the proposed mechanism, Masuda et al. suggested that the interaction between triethylamine and pinacolborane would furnish an ammonium/boride ion pair [Et₃NH⁺ · B-(OR)₂], in which the boride acts as the active transmetalating anion (Scheme 1). However, it is commonly accepted that the hydrogen atom in H-Bpin is hydridic rather than protonic, a result of the fact that the electronegativity of H is greater than that of B (indeed it is between that of B and C). Therefore, we suspected that it is highly unlikely for pinacolborane to protonate triethylamine to give a triethylammonium salt of a boryl anion.¹⁰ In 2003, Alcaraz et al.

*Corresponding authors. E-mail: todd.marder@durham.ac.uk; chzlin@ust.hk.

(1) (a) Suzuki, A. *Pure Appl. Chem.* **1994**, 66, 213. (b) Suzuki, A. *Pure Appl. Chem.* **1991**, 63, 419. (c) Matteson, D. S. *Tetrahedron* **1989**, 45, 1859. (d) Suzuki, A. *Pure Appl. Chem.* **1985**, 57, 1749. (e) Suzuki, A.; Miyaura, N. *Chem. Rev.* **1995**, 95, 2457. (f) Maezaki, N.; Sawamoto, H.; Yoshigami, R.; Suzuki, T.; Tanaka, T. *Org. Lett.* **2003**, 5, 1345. (g) *Boronic Acids, Preparation and Applications in Organic Synthesis and Medicine*; Hall, D. G., Ed.; Wiley-VCH Verlag GmbH & Co., KGaA: Weinheim, 2005.

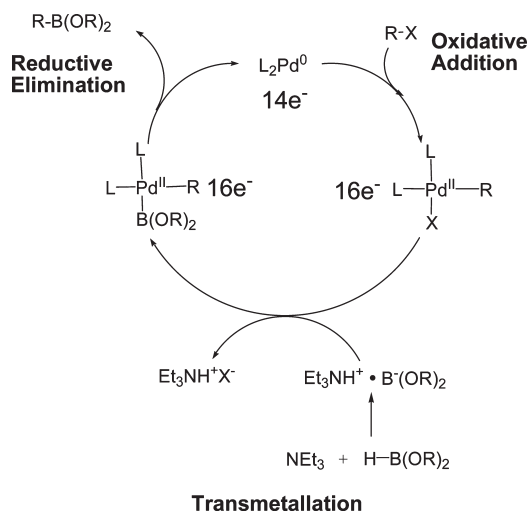
(2) (a) Matteson, D. S. In *The Chemistry of the Metal-Carbon Bond*; Hartley, F. R., Patai, S., Eds.; Wiley: New York, 1987; Vol. 4, pp 307–499. (b) Nesmeyanov, A. N.; Sokolik, R. A. *Methods of Elemento-Organic Chemistry*; North-Holland: Amsterdam, The Netherlands, 1967; Vol. 1.

(3) Zhu, L.; Duquette, J.; Zhang, M. *J. Org. Chem.* **2003**, 68, 3729.

(4) Mkhaliid, I. A. I.; Barnard, J. H.; Marder, T. B.; Murphy, J. C.; Hartwig, J. F. *Chem. Rev.* **2010**, 110, 890.

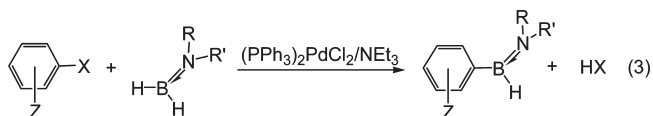
(5) Tsuji, J. *Palladium Reagents and Catalysts: New Perspectives for the 21st Century*; Wiley: Chichester, 2004.

Scheme 1



examined this proposed hypothesis by adding different amounts of triethylamine to H-Bpin and R_2N-BH_2 (R = alkyl), respectively.¹¹ They observed neither ionic nor Lewis acid–base interactions by *in situ* ^{11}B and ^{14}N NMR spectroscopy. Clearly, an alternative mechanism must account for the catalytic reactions.

In this theoretical work, we examined a new mechanism together with the one proposed by Masuda et al. Alcaraz et al. have also developed a novel and efficient way to prepare monomeric aryl(dialkylamino)boranes $ArB(H)-NRR'$ using (dialkylamino)boranes BH_2-NRR' (R and R' = alkyl) with Pd catalysts (eq 3).¹¹ Applying the new mechanism, we also investigated these recently reported catalytic reactions.



(6) (a) Ishiyama, T.; Murata, M.; Miyaura, N. *J. Org. Chem.* **1995**, 60, 7508. See also: (b) Ishiyama, T.; Itoh, Y.; Kitano, T.; Miyaura, N. *Tetrahedron Lett.* **1997**, 38, 3447. (c) Ishiyama, T.; Ishida, K.; Miyaura, N. *Tetrahedron* **2001**, 57, 9813. (d) Fürstner, A.; Seide, G. *Org. Lett.* **2002**, 4, 541. (e) Xu, C.; Gong, J.-F.; Song, M.-P.; Wu, Y.-J. *Transition Met. Chem.* **2009**, 34, 175.

(7) (a) Murata, M.; Oyama, T.; Watanabe, S.; Masuda, Y. *J. Org. Chem.* **2000**, 65, 164. (b) Murata, M.; Watanabe, S.; Masuda, Y. *J. Org. Chem.* **1997**, 62, 6458. See also: (c) Baudoin, O.; Guénard, D.; Guéritte, F. *J. Org. Chem.* **2000**, 65, 9268. (d) Wolan, A.; Zaidlewicz, M. *Org. Biomol. Chem.* **2003**, 1, 3274.

(8) (a) Morgan, A. B.; Jurs, J. L.; Tour, J. M. *J. Appl. Polym. Sci.* **2000**, 76, 1257. (b) Rosen, B. M.; Huang, C.; Percec, V. *Org. Lett.* **2008**, 10, 2597. (c) Wilson, D. A.; Wilson, C. J.; Rosen, B. M.; Percec, V. *Org. Lett.* **2008**, 10, 4879. (d) Moldoveanu, C.; Wilson, D. A.; Wilson, C. J.; Corcoran, P.; Rosen, B. M.; Percec, V. *Org. Lett.* **2009**, 11, 4974. (e) For a stepwise borylation of PhBr promoted by Ni, see: Debashis, A.; Huffman, J. C.; Mindiola, D. J. *Chem. Commun.* **2007**, 4489.

(9) (a) Kleeborg, C.; Dang, L.; Lin, Z.; Marder, T. B. *Angew. Chem., Int. Ed.* **2009**, 48, 5350. (b) For a Cu-catalyzed process involving HBpin, see: Zhu, W.; Ma, D. *Org. Lett.* **2006**, 8, 261.

(10) For reports on a novel lithium salt of a boryl anion, see: (a) Segawa, Y.; Yamashita, M.; Nozaki, K. *Science* **2006**, 314, 113. (b) See also: Marder, T. B. *Science* **2006**, 314, 69. (c) Braunschweig, H. *Angew. Chem., Int. Ed.* **2007**, 46, 1946. (d) Segawa, Y.; Suzuki, Y.; Yamashita, M.; Nozaki, K. *J. Am. Chem. Soc.* **2008**, 130, 16069.

(11) Euzenat, L.; Horhant, D.; Riboudouille, Y.; Duriez, C.; Alcaraz, G.; Vaultier, M. *Chem. Commun.* **2003**, 2280.

Computational Details

Geometry optimizations have been performed at the Becke3LYP (B3LYP) level of density functional theory.¹² To reduce computational costs, the bidentate phosphine ligand diphenylphosphinoferrocene (dppf), employed experimentally, was replaced by the model ligand diphenylphosphinopropane (dhpp = $PH_2CH_2CH_2CH_2PH_2$), in which the phenyl groups in dppf were replaced by H atoms. As the average ligand bite angle of dhpp (91°) is similar to that of dppf (96°),¹³ calculations using the model catalyst should give reasonable results. Triethylamine (NEt_3) was modeled by trimethylamine (NMe_3) and the monodentate phosphine ligand triphenylphosphine (PPh_3) was modeled by trimethylphosphine (PMe_3) to reduce the computational cost. In our calculations, we used H-Beg₂ ($eg_2 = OCH_2CH_2O$) as a model for pinacolborane, H-Bpin ($pin = OCMe_2CMe_2O$), in which the methyl groups were replaced by H atoms. The effective core potentials (ECPs) of Hay and Wadt with a double- ζ valence basis set (LanL2DZ)¹⁴ were used in describing Pd, P, and I, whereas the 6-31G basis set was used for all other atoms.¹⁵ Polarization functions were added for Pd ($\zeta_r = 1.472$)¹⁶ and those atoms that are directly bonded to the metal center, P ($\zeta_d = 0.340$), I ($\zeta_d = 0.266$), N ($\zeta_d = 0.864$), C ($\zeta_d = 0.600$), and B ($\zeta_d = 0.388$).¹⁷ Frequency calculations were carried out to confirm the characteristics of all of the optimized structures as minima or transition states. Calculations of intrinsic reaction coordinates (IRC) were also performed to confirm that the transition states connect the two corresponding minima.¹⁸ All calculations were performed with the Gaussian 03 software package.¹⁹ In studying the stability of the ammonium/boride ion pair, we carried out single-point solvation energy calculations with Gaussian 03 using the IEF-PCM model²⁰ using dioxane with a permittivity of 2.2 as the solvent.

For convenience in our discussion, all calculated structures of reactants and intermediates are numbered. The numbers are then followed by a bold letter **b** for those species having a bidentate phosphine ligand and **m** for those species having monodentate phosphine ligands. For each cationic species, a “+” symbol is added. Relative free energies are used because intermolecular reactions are considered and the entropy contribution is important.

Results and Discussion

In the mechanism (Scheme 1) proposed by Masuda et al., the boride in the ammonium/boride ion pair $[Et_3NH^+ \cdot B(OR)_2^-]$ is the active transmetalating anion. To study the

(12) (a) Becke, A. D. *Phys. Rev. A* **1988**, 38, 3098. (b) Miehlich, B.; Savin, A.; Stoll, H.; Preuss, H. *Chem. Phys. Lett.* **1989**, 157, 200. (c) Lee, C.; Yang, W.; Parr, G. *Phys. Rev. B* **1988**, 37, 785. (d) Becke, A. D. *J. Chem. Phys.* **1993**, 98, 5648.

(13) Dierkes, P.; van Leeuwen, P. W. N. M. *J. Chem. Soc., Dalton Trans.* **1999**, 1519.

(14) (a) Hay, P. J.; Wadt, W. R. *J. Chem. Phys.* **1985**, 82, 270. (b) Wadt, W. R.; Hay, P. J. *J. Chem. Phys.* **1985**, 82, 284. (c) Hay, P. J.; Wadt, W. R. *J. Chem. Phys.* **1985**, 82, 299.

(15) (a) Gordon, M. S. *Chem. Phys. Lett.* **1980**, 76, 163. (b) Hariharan, P. C.; Pople, J. A. *Theor. Chim. Acta* **1973**, 28, 213. (c) Binning, R. C., Jr.; Curtiss, L. A. *J. Comput. Chem.* **1990**, 11, 1206.

(16) Ehlers, A. W.; Bohme, M.; Dapprich, S.; Gobbi, A.; Hollwarth, A.; Jonas, V.; Kohler, K. F.; Stegmann, R.; Veldkamp, A.; Frenking, G. *Chem. Phys. Lett.* **1993**, 208, 111.

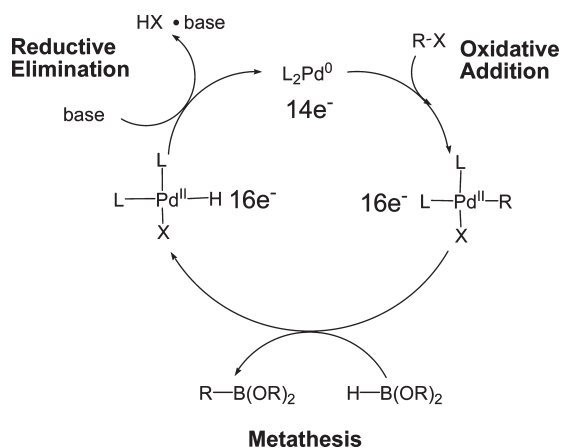
(17) Huzinaga, S. *Gaussian Basis Sets for Molecular Calculations*; Elsevier Science: Amsterdam, The Netherlands, 1984.

(18) (a) Fukui, K. *J. Phys. Chem.* **1970**, 74, 4161. (b) Fukui, K. *Acc. Chem. Res.* **1981**, 14, 363.

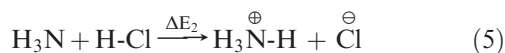
(19) Frisch, M. J.; et al. *Gaussian 03, Revision B.05*; Gaussian, Inc.: Wallingford, CT, 2004.

(20) (a) Cancès, M. T.; Mennucci, B.; Tomasi, J. *J. Chem. Phys.* **1997**, 107, 3032. (b) Cossi, M.; Barone, V.; Mennucci, B.; Tomasi, J. *Chem. Phys. Lett.* **1998**, 286, 253. (c) Mennucci, B.; Tomasi, J. *J. Chem. Phys.* **1997**, 106, 5151. (d) Cossi, M.; Scalmani, G.; Rega, N.; Barone, V. *J. Chem. Phys.* **2002**, 117, 43.

Scheme 2

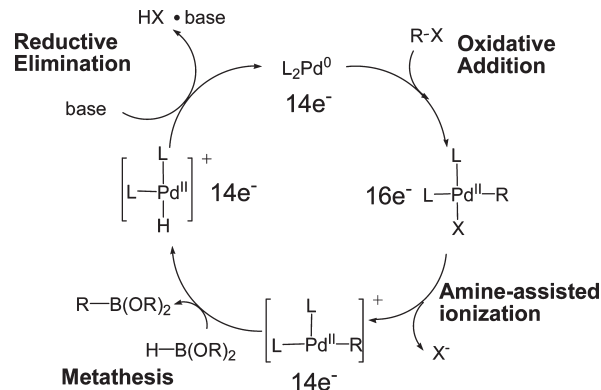


stability of such an ammonium/boride ion pair, we calculated the reaction energy of eq 4 both in the gas phase (ΔE_{1g}) and in solution (ΔE_{1s}) using dioxane as the solvent. ΔE_{1g} has a value of 187.14 kcal/mol. Even with inclusion of the solvation energies, the reaction is extremely endothermic, with $\Delta E_{1s} = 129.28$ kcal/mol. To validate the reliability of the PCM solvation model used in our solvation energy calculations, we calculated ΔE_2 for the reaction given by eq 5. The reaction energy in the gas phase (ΔE_{2g}) was calculated to be 116.77 kcal/mol, while ΔE_{2s} , using water as the solvent, was calculated to be -28.65 kcal/mol, which is negative. This result is consistent with the experimental observation that ammonium and chloride ions are stable in water because of their large solvation energies. The large positive reaction energy (ΔE_1) calculated for eq 4 implies that the ammonium/boride ion pair is highly unstable. The results of these calculations indicate that the formation of an ammonium/boride ion pair is unfeasible.



An alternative mechanism must account for the catalytic reactions and, although a neutral process is conceivable (Scheme 2), we suggest that it involves the metathesis process $[\text{L}_n\text{Pd-Ar}(\eta^2\text{-H-B(OR)}_2)]^+ \rightarrow [\text{L}_n\text{Pd-H}(\eta^2\text{-Ar-B(OR)}_2)]^+$, shown in Scheme 3.

Scheme 3



Calculated Energy Profiles for Scheme 2. Figure 1a shows the energy profiles for the mechanism proposed in Scheme 2, which includes three major stages: (i) oxidative addition of iodobenzene to the Pd(0) center; (ii) a metathesis process via a four-center transition state; and (iii) regeneration of the active species. Important structural parameters for the B3LYP-optimized intermediates and transition states calculated for this mechanism are summarized in Figure 2.

First, oxidative addition of iodobenzene to the Pd(0) complex (η^2 -dhpp)Pd(0) **1b** (dhpp = dihydridophosphino-propane) was investigated theoretically.²¹ Two reaction pathways are possible. Path A involves dissociation of one arm of the bidentate ligand followed by oxidative addition of iodobenzene to the palladium center. The active Pd(0) complex **1b** has a Pd–P bond distance of 2.301 Å. From (η^2 -dhpp)Pd **1b**, partial ligand dissociation occurs via the transition state **TS**_{1b–2b} to afford (η^1 -dhpp)Pd **2b**. From **2b**, iodobenzene coordinates with the Pd center to give a σ -complex, (η^1 -dhpp)Pd(η^2 -Ph-I) **3b**, which then undergoes oxidative addition via **TS**_{3b–4b} to afford a three-coordinate species, *cis*-Pd-(Ph)(I)(η^1 -dhpp) **4b**. Complex **4b** adopts a T-shaped structure, with the phenyl ligand and the coordinated arm of the bidentate ligand being *trans* to one another. Due to the strong *trans* influence of the phenyl ligand, the Pd–P bond (2.473 Å) *trans* to it is longer than that of **1b** (Pd–P 2.301 Å). As **4b** is a coordinatively unsaturated species, HBpin can coordinate with the Pd center to yield the σ -borane complex **5b**, (η^1 -dhpp)Pd(Ph)(I)(η^2 -H-Bpin), a species ready for σ -bond metathesis.

Path B involves oxidative addition of iodobenzene directly with **1b**. From (η^2 -dhpp)Pd **1b**, iodobenzene easily coordinates with the Pd center to give a σ -complex, (η^2 -dhpp)Pd-(η^2 -Ph-I) **9b**. Oxidative addition of iodobenzene in **9b** affords the square-planar Pd(II) complex *cis*-Pd-(Ph)(I)(η^2 -dhpp) **10b** via the transition state **TS**_{9b–10b}. In **10b**, the Pd–P bond (2.426 Å) *trans* to Ph is longer than that of **1b** (Pd–P = 2.301 Å); the other Pd–P bond (2.312 Å) is shorter. After the oxidative addition, ligand dissociation leads to the neutral T-shape Pd(II) species **4b**, *cis*-Pd-(Ph)(I)(η^1 -dhpp).

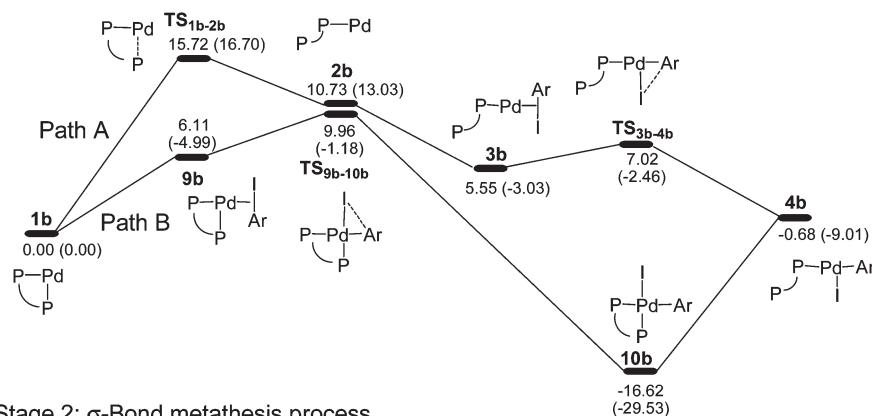
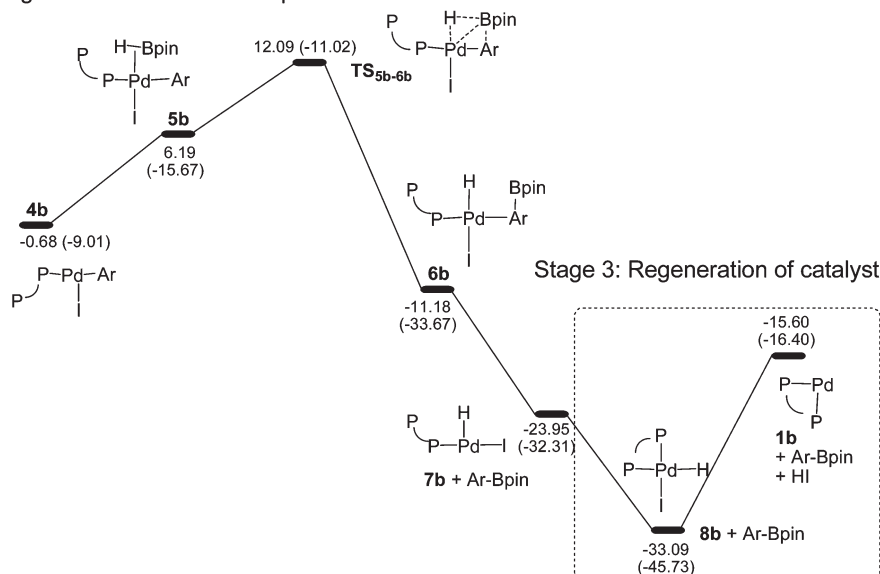
The second stage begins with **4b**. Pinacolborane coordinates to the Pd center of **4b** to yield the σ -borane complex **5b**. In **5b**, the boryl group of pinacolborane is pointing toward the phenyl ligand. The H–B bond distance (1.222 Å) represents a normal elongation for a σ -borane complex,²² by

(21) (a) Portnoy, M.; Milstein, D. *Organometallics* **1993**, *12*, 1665. (b) Kranenburg, M.; Kamer, P. C. J.; van Leeuwen, P. W. N. M.; Vogt, D.; Keim, W. *J. Chem. Soc., Chem. Commun.* **1995**, 2177. (c) Sakaki, S.; Biswas, B.; Sugimoto, M. *J. Chem. Soc., Dalton Trans.* **1997**, 803. (d) Su, M.; Chu, S. *Inorg. Chem.* **1998**, *37*, 3400. (e) Sundermann, A.; Uzan, O.; Martin, J. M. L. *Chem.–Eur. J.* **2001**, *7*, 1703. (f) Lin, B. L.; Liu, L.; Fu, Y.; Luo, S. W.; Chen, Q.; Guo, Q. X. *Organometallics* **2004**, *23*, 2114. (g) Senn, H. M.; Ziegler, T. *Organometallics* **2004**, *23*, 2980. (h) Kozuch, S.; Shaik, S.; Jutand, A.; Amatore, C. *Chem.–Eur. J.* **2004**, *10*, 3072. (i) Kozuch, S.; Amatore, C.; Jutand, A.; Shaik, S. *Organometallics* **2005**, *24*, 2319. (j) Ahlquist, M.; Fristrup, P.; Tanner, D.; Norrby, P.-O. *Organometallics* **2006**, *25*, 2066. (k) Fairlamb, I. J. S.; O'Brien, C. T.; Lin, Z.; Lam, K. C. *Org. Biomol. Chem.* **2006**, *4*, 1213. (l) Legault, C. Y.; Garcia, Y.; Merlic, C. A.; Houk, K. N. *J. Am. Chem. Soc.* **2007**, *129*, 12664. (m) Lam, K. C.; Marder, T. B.; Lin, Z. *Organometallics* **2007**, *26*, 758. (n) de Jong, G. T.; Bickelhaupt, F. M. *ChemPhysChem* **2007**, *8*, 1170. (o) de Jong, G. T.; Bickelhaupt, F. M. *J. Chem. Theory Comput.* **2007**, *3*, 514. (p) Li, Z.; Fu, Y.; Guo, Q.-X.; Liu, L. *Organometallics* **2008**, *27*, 4043. (q) van Zeist, W.-J.; Visser, R.; Bickelhaupt, F. M. *Chem.–Eur. J.* **2009**, *15*, 6112. (r) de Jong, G. T.; Bickelhaupt, F. M. *Can. J. Chem.* **2009**, *87*, 806.

(22) Aldridge, S.; Calder, R. J.; Rossin, A.; Dickinson, A. A.; Willock, D. J.; Jones, C.; Evans, D. J.; Steed, J. W.; Light, E. M.; Coles, S. J.; Hursthouse, M. B. *J. Chem. Soc., Dalton Trans.* **2002**, 2020.

(a) Neutral pathway

Stage 1: Oxidative addition

Stage 2: σ -Bond metathesis process

Stage 3: Regeneration of catalyst

(b) Cationic pathway

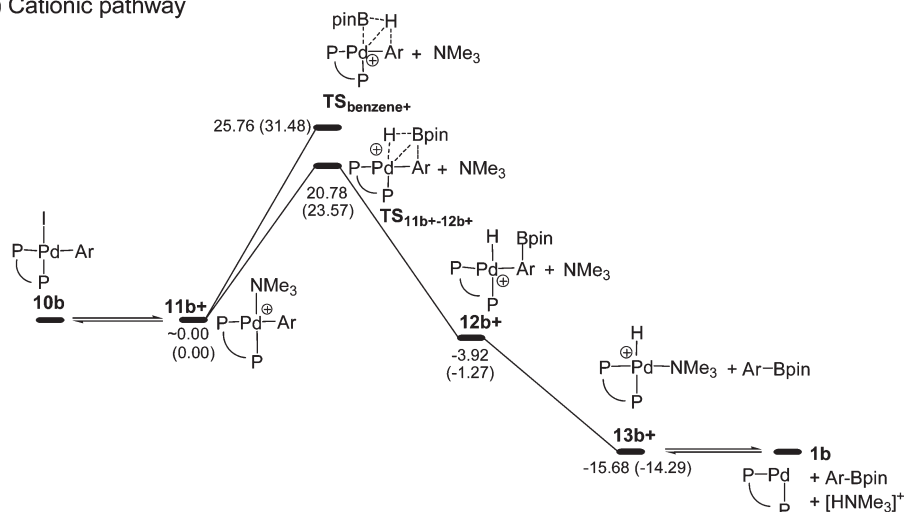


Figure 1. (a) Energy profiles on the basis of the reaction mechanism proposed in Scheme 2. (b) Energy profiles for a new reaction mechanism involving a cationic complex. The calculated relative free energies and electronic energies (in parentheses) are given in kcal/mol.

comparison with the calculated H–B bond distance of 1.186 Å in free pinacolborane. This is actually at the shorter end of the measured values of 1.24(2)–1.35(3) Å from X-ray

diffraction, although a continuum might exist between borane and boryl hydride structures.²³ The metathesis process of $(\eta^1\text{-dhpp})\text{Pd}(\text{I})(\text{Ph})(\eta^2\text{-H-Bpin})$ **5b** \rightarrow $(\eta^1\text{-dhpp})\text{Pd}(\text{I})(\text{H})(\text{Ph-Bpin})$

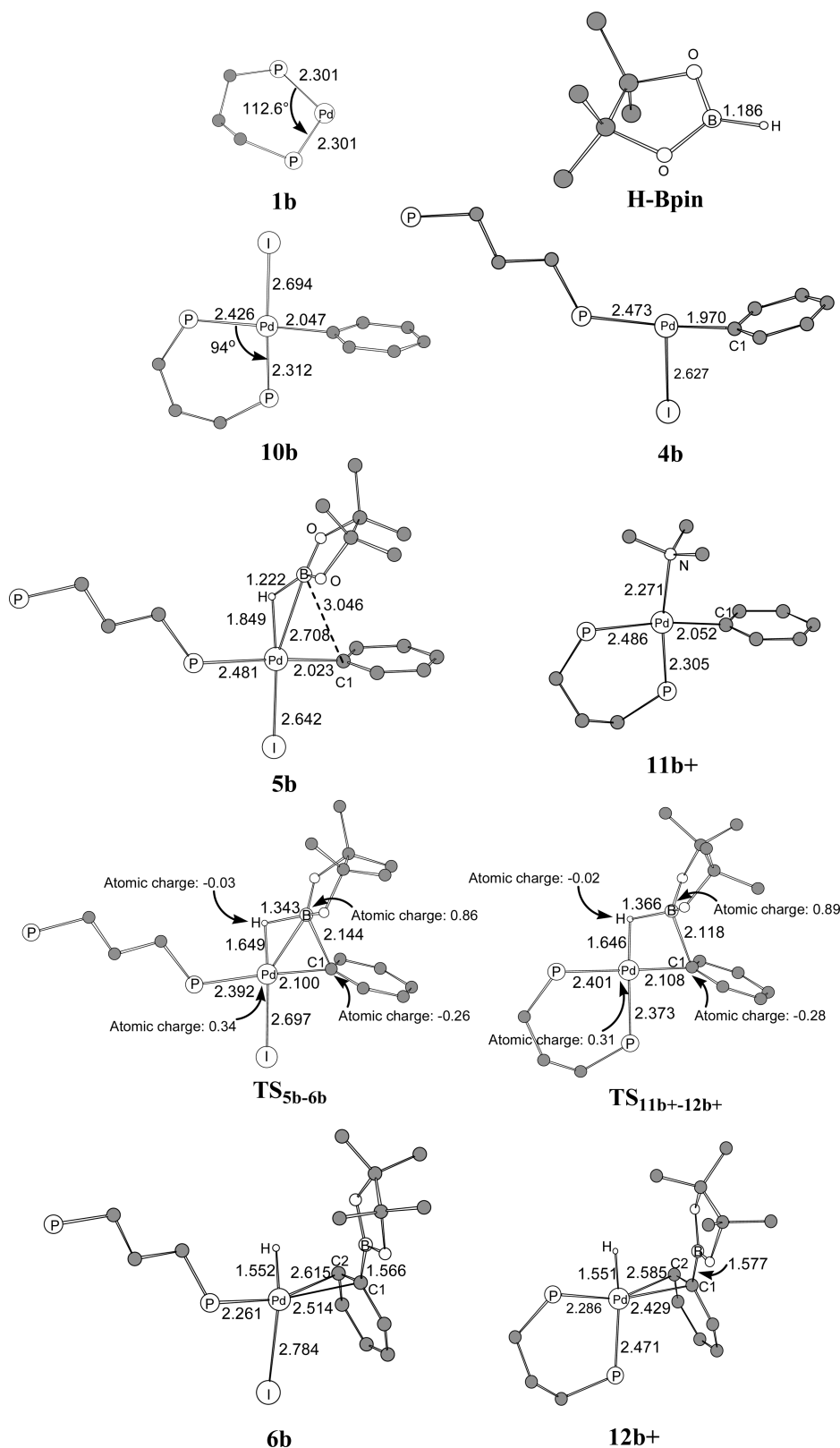


Figure 2. B3LYP optimized structures for those species shown in Figure 1 together with selected bond distances and angles given in Å and deg, respectively. For the purpose of clarity, hydrogen atoms on the methyl groups, phenyl groups, and bidentate phosphine ligand (dhpp) are omitted. Atomic charges on selected atoms in TS_{5b-6b} and TS_{11b+-12b+} are also given.

6b proceeds via a four-center transition state, TS_{5b-6b}, which involves breaking of the H–B bond and concerted B–C1

bond formation. The most pronounced structural changes from **5b** to TS_{5b-6b} are the lengthening of the H–B bond to 1.343 Å, indicating the importance of H–B bond breaking, and the shortening of the B–C1 distance to 2.144 Å, indicating

formation of the B–C bond. In **6b**, (η^1 -dhpp)Pd(I)(H)(Ph-Bpin), the phenyl plane of Ph-Bpin is almost parallel with the Pd–H bond. The Pd–C1 and Pd–C2 bonds (Figure 2) are calculated to be 2.514 and 2.615 Å, respectively, suggesting that the π orbitals of the phenyl group interact with the unoccupied $d\sigma$ orbital of the Pd center.²⁴ The next step is elimination of the phenylborane Ph-Bpin from **6b** to afford the three-coordinate T-shaped Pd(II) species **7b**, *cis*-(Pd)(H)(I)-(η^1 -dhpp).

In the final stage, the uncoordinated end of the dhpp ligand coordinates to the Pd center to afford the four-coordinate Pd complex **8b**, (η^2 -dhpp)Pd(H)(I). Elimination of HI from **8b** with the aid of base regenerates the 14-electron complex (η^2 -dhpp)Pd **1b** and completes the catalytic cycle.

On the basis of the energetics shown in Figure 1, we can see that **10b**, which can be easily formed via path B, is a thermodynamic sink. Even via path A, once formed, **4b** is immediately transformed into **10b** and does not have a chance to undergo the σ -bond metathesis in the second stage because **4b** \rightarrow **10b** is barrierless. Therefore, the overall barrier of the rate-determining step for the proposed reaction mechanism is 28.71 kcal/mol from **10b** to **TS**_{5b–6b}. The barrier is clearly high.²⁵ Therefore, the reaction from the neutral complex **10b** (a neutral pathway) is probably not the best.

Reaction Mechanism Involving a Cationic Complex. We propose here a cationic pathway for the σ -bond metathesis process, as shown in Figure 1b. Replacing the iodide ligand in **10b** with trimethylamine, NMe₃, would afford the cationic complex [*cis*-Pd(Ph)(NMe₃)(η^2 -dhpp)]⁺ **11b**⁺. In 1991, Trogler et al. reported the single-crystal X-ray structure of the cationic complex [PdMe(NEt₃)(η^2 -dppe)]⁺,²⁶ and Cabri et al. observed similar neutral and cationic Pd(II) complexes in Heck reactions.^{27,28} Amatore et al. reported the equilibrium constant (*K*_i) for the ionization reaction in DMF, Pd(Ph)(I)(PPh₃)₂ \rightarrow Pd(Ph)(PPh₃)₂⁺ + I[–]. With the value of *K*_i [PdPhIL₂/[PhPdL₂⁺][I[–]] = 1.5 \times 10³ M^{–1}], the ion pair is 4.33 kcal/mol higher in free energy than the neutral species.²⁹ Rösch et al. also proposed a cationic pathway for the Heck reactions they studied.³⁰ All of these experimental and theoretical results indicate that the proposed cationic pathway for the catalytic process is feasible.

The cationic pathway begins with the cationic complex **11b**⁺. The aforementioned equilibrium constant value indicates that the energy difference between Pd(Ph)(I)(PPh₃)₂ and the ion pair [Pd(Ph)(PPh₃)₂]⁺ + [I][–] in a basic, polar

solvent is not large. For the convenience of our discussion, we set **10b** and **11b**⁺ at the same energy level (Figure 1b), realizing that DFT calculations will overestimate the energies of any charge-separated species. The Pd–P bond *trans* to NMe₃ in **11b**⁺ has a bond length of 2.305 Å. The replacement of iodide with NMe₃ has only a minor effect on the Pd–P bond length, both being weak *trans*-influence ligands. In the transition state for the metathesis process, **TS**_{11b⁺–12b⁺}, H-Bpin lies almost in the coordination plane of the Pd center with the boryl group of pinacolborane pointing toward the phenyl ligand. From **11b**⁺ to **TS**_{11b⁺–12b⁺}, the B–C distance shortens to 2.118 Å and the H–B bond lengthens to 1.366 Å. **TS**_{11b⁺–12b⁺} is a concerted four-center transition state. The Pd–C1 and Pd–C2 bonds in the cationic complex **12b**⁺ are calculated to be 2.429 and 2.585 Å, respectively, which are slightly shorter than the corresponding Pd–C bonds in the neutral complex **6b** (Pd–C1 = 2.514 Å and Pd–C2 = 2.615 Å). After elimination of phenylborane Ph-Bpin from **12b**⁺, NMe₃ recoordinates to the Pd center to yield the cationic Pd(II) complex **13b**⁺, [(η^2 -dhpp)-Pd(H)(NMe₃)]⁺. Deprotonation of **13b**⁺ regenerates the 14-electron complex (η^2 -dhpp)Pd **1b** with the aid of the base, NMe₃, completing the catalytic cycle. Leoni et al. examined the acidic behavior of *trans*-[(Cy₃P)₂Pd(H)(H₂O)]⁺BF₄[–] with Et₃N and observed that deprotonation gives (Cy₃P)₂Pd in high yield.³¹

By comparing the energetics of the neutral and cationic pathways, one finds that the cationic pathway is favored over the neutral one. The activation barrier of 20.78 kcal/mol is moderate, consistent with the reaction temperature of 80 °C. It is important to note that the experiments conducted by both Masuda et al.⁷ and Alcaraz et al.¹¹ show that electron-donating substituents on the aryl halide substrates promote their catalytic reactions. This is unusual for many cross-coupling reactions,³² in which oxidative addition of aryl halide is often rate-determining. It is expected that electron-rich aryl ligands and electron-deficient metal centers favor the σ -bond metathesis process. In the transition states **TS**_{11b⁺–12b⁺} and **TS**_{5b–6b}, the H–B distance in **TS**_{11b⁺–12b⁺} is longer but the B–C distance shorter when compared with those in **TS**_{5b–6b}, suggesting that the H–B bond breaking and the B–C bond formation are more favorable in the cationic pathway than in the neutral pathway. The calculated NBO natural charges³³ of selected atoms in **TS**_{11b⁺–12b⁺} and **TS**_{5b–6b} are also shown in Figure 2. Boron is more positive and C1 is more negative in the cationic transition state in comparison with the neutral transition state.

Comments on the Formation of the Undesirable Hydrodehalogenation Byproduct. In the **TS**_{11b⁺–12b⁺} transition-state structure shown in Figure 2, the boryl group is pointing toward the phenyl ligand. With this configuration, the desirable product, phenylborane Ph-Bpin, is obtained. However, the alignment of pinacolborane can be reversed in such a way that the hydride points toward the phenyl ligand. With this reversed configuration, the undesirable hydrodehalogenation byproduct, benzene, is obtained along with a Pd-Bpin species. The transition state for the formation of benzene **TS**_{benzene⁺} in the cationic pathway was calculated

(24) Biswas, B.; Sugimoto, M.; Sakaki, S. *Organometallics* **2000**, *19*, 3895.

(25) Scudder, P. H. *Electron Flow in Organic Chemistry*; John Wiley & Sons: New York, 1992; p 40.

(26) Seligson, A. L.; Trogler, W. C. *J. Am. Chem. Soc.* **1991**, *113*, 2520.

(27) (a) Cabri, W.; Candiani, I.; Bedeschi, A.; Penco, S. *J. Org. Chem.* **1992**, *57*, 1481. (b) Cabri, W.; Candiani, I. *Acc. Chem. Res.* **1995**, *28*, 2.

(28) (a) For a review, see: Knowles, J. P.; Whiting, A. *Org. Biomol. Chem.* **2007**, *5*, 31. For selected theoretical studies, see: (b) Albert, K.; Gisdakis, P.; Rösch, N. *Organometallics* **1998**, *17*, 1608. (c) Deeth, R. J.; Smith, A.; Brown, J. M. *J. Am. Chem. Soc.* **2004**, *126*, 7144. (d) Lee, M.-T.; Lee, H. M.; Hu, C.-H. *Organometallics* **2007**, *26*, 1317. (e) Surawatanawong, P.; Fan, Y.; Hall, M. B. *J. Organomet. Chem.* **2008**, *693*, 1552. (f) Surawatanawong, P.; Hall, M. B. *Organometallics* **2008**, *27*, 622. (g) Henriksen, S. T.; Norrby, P. O.; Kaukoranta, P.; Andersson, P. G. *J. Am. Chem. Soc.* **2008**, *130*, 10414.

(29) Amatore, C.; Carré, E.; Jutand, A.; M'Barki, M. A.; Meyer, G. *Organometallics* **1995**, *14*, 5605.

(30) Albert, K.; Gisdakis, P.; Rösch, N. *Organometallics* **1998**, *17*, 1608.

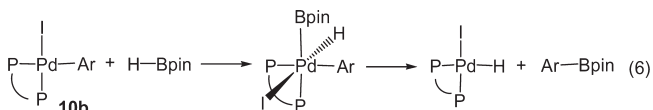
(31) Leoni, P.; Sommovigo, M.; Pasquali, M.; Midollini, S.; Braga, D.; Sabatino, P. *Organometallics* **1991**, *10*, 1038.

(32) Diederich, F.; Stang, P. J. *Metal-catalyzed Cross-coupling Reactions*; Wiley: New York, 1998.

(33) Glendening, E. D.; Reed, A. E.; Carpenter, J. E.; Weighold, F. *NBO, Version 3.1*.

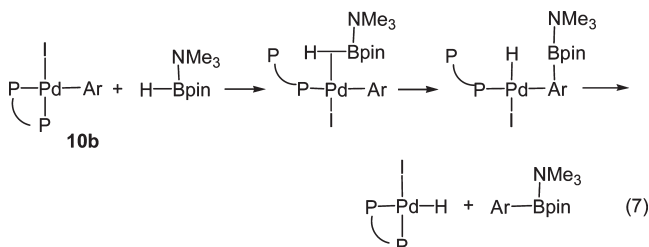
to be 4.98 kcal/mol higher in free energy than the transition state $\text{TS}_{11\text{b}+12\text{b}+}$. The results explain the experimental observation that the arene byproduct was obtained in some cases. $\text{TS}_{11\text{b}+12\text{b}+}$ is lower in energy than $\text{TS}_{\text{benzene}+}$, most likely due to a favorable charge matching between the $\text{B}^{\delta+}-\text{H}^{\delta-}$ and $\text{Pd}^{\delta+}-\text{Ph}^{\delta-}$ bonds.

Other Mechanistic Considerations for the Metathesis Process. After studying the mechanisms involving σ -bond metathesis, one may consider the possibility of an alternative pathway involving oxidative addition of pinacolborane to a Pd(II) center to give a Pd(IV) intermediate followed by reductive elimination of Ar-Bpin, as shown in eq 6. Starting from *cis*-Pd-(Ph)(I)(η^2 -dhpp) **10b**, pinacolborane could oxidatively add to the Pd center to afford the Pd(IV) intermediate (H)(Bpin)Pd(Ph)(I)(η^2 -dhpp). This Pd(IV) intermediate is found to be very unstable, being 37.49 kcal/mol higher in free energy than **10b**. The instability of the Pd(IV) intermediate is probably due to the fact that Pd does not favor a high oxidation state with the ligand environment present in this system. Even with the more electron-donating bidentate phosphine ligand dmpp ($\text{PMe}_2\text{CH}_2\text{CH}_2\text{CH}_2\text{PMe}_2$), the Pd(IV) intermediate is still computed to be very unstable. The energy difference between **10b** and the corresponding Pd(IV) intermediate is 39.94 kcal/mol when dmpp was used as the bidentate ligand. Here, steric factors seem to be rather important. The highly unstable intermediate eliminates the possibility of a Pd(II)–Pd(IV) mechanism.



We have also examined another reaction path starting from *cis*-Pd-(Ph)(I)(κ^2 -dhpp) **10b**. Although unlikely, reaction of pinacolborane with trimethylamine could conceivably generate an adduct $\text{HBpin}\cdot\text{NMe}_3$. The B–N bond distance in the adduct was calculated to be 1.714 Å, longer than those found (1.64–1.66 Å) in the X-ray crystal structures of $\text{MeBcat}\cdot\text{py}$ and $\text{ClBcat}\cdot\text{NEt}_3$.^{34,35} A longer B–N distance calculated for the adduct is expected because HBpin is a weaker Lewis acid than either MeBcat or ClBcat. Using this adduct in place of free HBpin as a substrate for the metathesis process is shown in eq 7, and the corresponding metathesis transition state related to this process was found to be 24.48 kcal/mol higher in free energy than the transition state $\text{TS}_{5\text{b}-6\text{b}}$ in the neutral pathway. Clearly, the pathway using the borane-amine adduct as a substrate for the metathesis can also be eliminated. Again, we note that Alcaraz et al.¹¹ found no evidence

for adduct formation when HBpin and Et_3N were mixed (*vide supra*).



Catalytic Reactions of Eq 3. Applying the newly proposed mechanism involving a cationic pathway, we investigated the catalytic reactions for the synthesis of the monomeric aryl(dialkylamino)boranes $\text{Ar}(\text{H})\text{B-NR}_1\text{R}_2$ using the (dialkylamino)boranes $\text{BH}_2\text{-NR}_1\text{R}_2$ (R_1 and R_2 = alkyl) as the substrates in a process catalyzed by monodentate phosphine-containing Pd complexes (eq 3).¹¹

Figure 3 shows the energy profiles for the catalytic reactions on the basis of the newly proposed cationic reaction mechanism discussed above. Three major stages were considered: (i) oxidative addition of iodobenzene to the Pd(0) center; (ii) a metathesis process via a four-center transition state; and (iii) regeneration of the active species. Important structural parameters for selected B3LYP-optimized intermediates and transition states are summarized in Figure 4.

First, oxidative addition of iodobenzene to $(\text{PMe}_3)_2\text{Pd}(0)$ **1m** was investigated theoretically. Again, there are two possible reaction pathways.^{21m} Path C involves dissociation of one of the two phosphine ligands followed by oxidative addition of iodobenzene to the palladium center. The active species Pd(0) complex $(\text{PMe}_3)_2\text{Pd}$ **1m** dissociates one of the phosphine ligands to afford $(\text{PMe}_3)\text{Pd}$ **2m**. From **2m**, iodobenzene coordinates with the Pd center to give a σ -complex, $(\text{PMe}_3)\text{Pd}(\eta^2\text{-Ph-I})$ **3m**, which then undergoes oxidative addition via $\text{TS}_{3\text{m}-4\text{m}}$ to afford a three-coordinate species, *cis*-Pd-(Ph)(I)(PMe_3) **4m**. As **4m** is a coordinatively unsaturated species, the phosphine ligand can coordinate to the Pd center to give a four-coordinate Pd(II) complex, *cis*-Pd-(Ph)(I)(PMe_3)₂ **5m**.

Path D involves oxidative addition of iodobenzene directly to **1m**, giving a Pd(II) complex, *cis*-Pd-(Ph)(I)(PMe_3)₂ **5m**, via the transition state $\text{TS}_{1\text{m}-5\text{m}}$. Complex **5m** is a four-coordinate square-planar Pd(II) complex, with the phenyl and iodide ligands being *cis* to each other. We have previously discussed the oxidative addition of ArX to $(\text{PMe}_3)_n\text{Pd}$ ($n = 1, 2$) in detail.^{21m} This species can isomerize to the more stable *trans* isomer **12m**.³⁶ After dissociation of one of the two phosphine ligands to give a neutral three-coordinate T-shaped *cis*-intermediate **9m**, in which the

(34) For $\text{RBcat}\cdot\text{amine}$ adducts, see, for example: (a) Clegg, W.; Scott, A. J.; Souza, F. E. S.; Marder, T. B. *Acta Crystallogr.* **1999**, c55, 1885. (b) Coapes, R. B.; Souza, F. E. S.; Fox, M. A.; Batsanov, A. S.; Goeta, A. E.; Yufit, D. S.; Leech, M. A.; Howard, J. A. K.; Scott, A. J.; Clegg, W.; Marder, T. B. *J. Chem. Soc., Dalton Trans.* **2001**, 1201. (c) Nguyen, P.; Dai, C. Y.; Taylor, N. J.; Power, W. P.; Marder, T. B.; Pickett, N. L.; Norman, N. C. *Inorg. Chem.* **1995**, 34, 4290. (d) Clegg, W.; Dai, C. Y.; Lawlor, F. J.; Marder, T. B.; Nguyen, P.; Norman, N. C.; Pickett, N. L.; Power, W. P.; Scott, A. J. *J. Chem. Soc., Dalton Trans.* **1997**, 839.

(35) We note that Bpin compounds are relatively poor Lewis acids. However, for exceptionally strong Lewis bases (e.g., RO^- , NHC) or tris-chelating moieties, adducts involving B_2pin_2 or RBpin are possible; see ref 9a and (a) Lee, K.-S.; Zhugralin, A. R.; Hoveyda, A. H. *J. Am. Chem. Soc.* **2009**, 131, 7253. (b) Gao, M.; Thorpe, S. B.; Santos, W. L. *Org. Lett.* **2009**, 11, 3478.

(36) (a) Wilkins, R. G. *Kinetics and Mechanism of Reactions of Transition Metal Complexes*, 2nd ed.; VCH: Weinheim, Germany, 1991; pp 356–359. (b) Casado, A. L.; Espinet, P. *Organometallics* **1998**, 17, 954. (c) Minniti, D. *Inorg. Chem.* **1994**, 33, 2631. (d) Alibrandi, G.; Minniti, D.; Sclaro, M. L.; Romeo, R. *Inorg. Chem.* **1988**, 27, 318. (e) Casado, A. L.; Casares, J. A.; Espinet, P. *Inorg. Chem.* **1998**, 37, 4154. (f) Basolo, F.; Pearson, G. *Mechanism of Inorganic Reactions*, 2nd ed.; Wiley: New York, 1967. (g) Anderson, G. K.; Cross, R. J. *J. Chem. Soc. Rev.* **1980**, 9, 185. (h) Berry, R. S. *J. Chem. Phys.* **1960**, 32, 933. (i) Ozawa, F.; Ito, T.; Nakamura, Y.; Yamamoto, A. *Bull. Chem. Soc. Jpn.* **1981**, 54, 1868. (j) Pavonessa, R. S.; Troglor, W. C. *J. Am. Chem. Soc.* **1982**, 104, 3529. (k) Goossen, L. J.; Koley, D.; Hermann, H. L.; Thiel, W. *Organometallics* **2005**, 24, 2398. (l) Morrell, D. G.; Kochi, J. K. *J. Am. Chem. Soc.* **1975**, 97, 7262. (m) Tasumi, K.; Nakamura, A.; Komiya, S.; Yamamoto, A.; Yamamoto, T. *J. Am. Chem. Soc.* **1984**, 106, 8181. (n) Komiya, S.; Albright, T. A.; Hoffmann, R.; Kochi, J. K. *J. Am. Chem. Soc.* **1976**, 98, 7255.

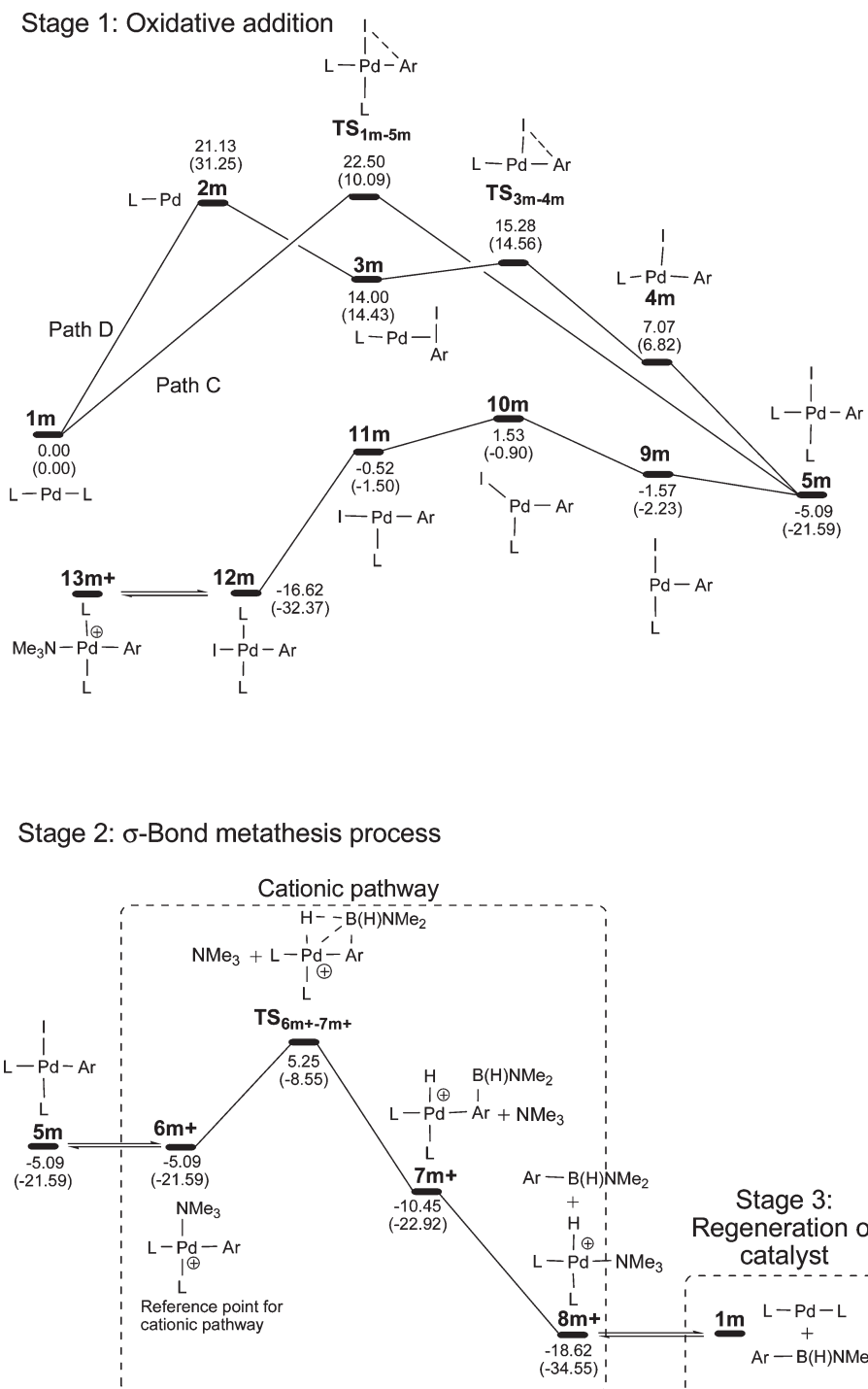


Figure 3. Energy profiles for the catalytic reactions shown in eq 3 on the basis of a cationic reaction mechanism. The calculated relative free energies and electronic energies (in parentheses) are given in kcal/mol. L = PMe₃.

vacant site is *trans* to the strong *trans*-influence aryl ligand, an interconversion to its *trans*-isomer **11m** takes place via the Y-shaped species **10m**. The phosphine ligand recoordinates to the Pd center of **11m** to afford **12m**. The barrier for the *cis*–*trans* isomerization process (**5m** → **12m**) is approximately 6.62 kcal/mol. Three different mechanisms are usually considered for the *cis*–*trans* isomerization in square-planar complexes: the associative pathway, the Berry pseudo-rotation mechanism, and the dissociative pathway.³⁶ Indeed, which is the most favorable depends on the nature of the solvent, the electronic effects of the ligands, and the

temperature. In this *cis*–*trans* isomerization process (**5m** → **12m**), we found that the dissociative pathway is the most favorable.

By replacing the iodide ligand in **5m** and **12m** with NMe₃, we obtain the cationic species **6m+** and **13m+**, respectively.^{28,30} Again, we set **5m** and **6m+** at the same energy level for convenience in our discussion. The cationic pathway begins with the cationic complex [*cis*-Pd(Ph)-(NMe₃)(PMe₃)₂]⁺ **6m+**. In the transition state for the metathesis process, TS_{6m+–7m+}, H–B(H)NMe₂ lies almost in the coordination plane of the Pd center, with the boryl group

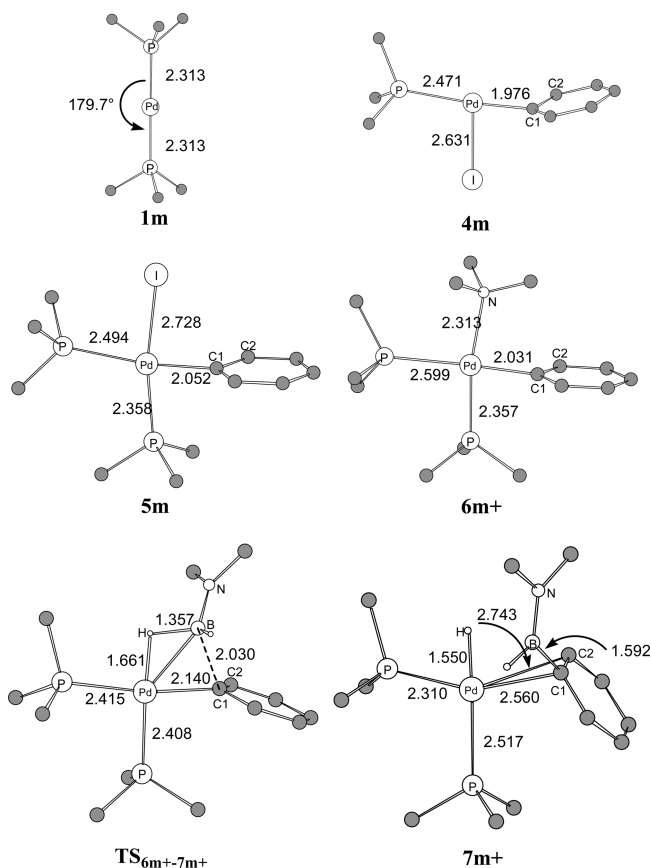


Figure 4. B3LYP optimized structures for those species shown in Figure 3 together with selected bond distances and angles given in Å and deg, respectively. For the purpose of clarity, hydrogen atoms on the methyl groups and phenyl groups are omitted.

pointing toward the phenyl ligand. From **6m+** to **TS_{6m+–7m+}**, the B–C distance shortens to 2.030 Å and the H–B bond lengthens to 1.357 Å. **TS_{6m+–7m+}** is a concerted, four-center transition state. The Pd–C1 and Pd–C2 distances in the cationic complex **7m+** are calculated to be 2.560 and 2.743 Å, respectively, suggesting that the π orbitals of the phenyl group interact with the unoccupied $d\sigma$ orbital of the Pd center.²⁴

After elimination of Ph-B(H)NMe₂ from **7m+**, NMe₃ recoordinates to the Pd center to yield the cationic Pd(II) complex **8m+**, [(PMe₃)₂(Pd)(H)(NMe₃)]⁺. Deprotonation of **8m+** regenerates the 14-electron species (PMe₃)₂Pd **1m** with the aid of NMe₃ as the base and completes the catalytic cycle.³¹

On the basis of the energetics shown in Figure 3, we can see that **12m** is a thermodynamic sink, similar to **10b**. Once **5m** is formed, it immediately isomerizes to **12m**. As **12m** has to isomerize to **5m** again in order to proceed with the σ -bond metathesis, the overall barrier to complete the σ -bond metathesis process is 21.87 kcal/mol from **12m** to **TS_{6m+–7m+}**. Therefore, both the oxidative addition process and the σ -bond metathesis process have similar energetics, and thus, either can be rate-determining. The electron-deficient aryl ligands and electron-rich metal centers favor the oxidative addition process, while the reverse situation favors the σ -bond metathesis process. The experiments conducted by Alcaraz et al.¹¹ show that donor substituents on the aryl ligand enhance the yield, suggesting that in this system the σ -bond metathesis is rate-determining.

Comments on the Different Catalytic Activities of Pd Catalysts Having Monodentate and Bidentate Phosphine Ligands. Masuda et al. reported Pd-catalyzed cross-coupling reactions using a bidentate phosphine ligand (eq 2).⁷ Alcaraz et al. used a Pd catalyst with monodentate phosphine ligands (eq 3).¹¹ From the calculation results, we found that the barrier for the oxidative addition process with a Pd catalyst having a bidentate phosphine ligand is lower than that for a Pd catalyst having monodentate phosphine ligands. This finding is consistent with those reported earlier that bidentate ligands with bite angles close to 90° promote oxidative addition of aryl halides to a Pd metal center.^{13,21}

Further Comments on the Role of Base. In many Pd-catalyzed carbon–carbon coupling reactions, bases are necessary, but their roles are different from one reaction to another.^{1e,29,32,37} In the catalytic reactions studied here, the base, NR₃, was found to play a dual role. NMe₃ is necessary to neutralize HX produced from the reaction of ArX + HBR₂ in order to regenerate the active Pd species. Through our studies, we believe that NR₃ also helps the catalytic reactions to proceed via a cationic reaction pathway by coordinating to the cationic Pd intermediate, thereby enhancing halide dissociation. Thus, we propose that alternative and more coordinating bases, such as pyridine derivatives, may promote the reaction even more effectively than Et₃N, and experimental studies of this are in progress.³⁸

Conclusions

The Pd-catalyzed borylation of aryl halides using HBpin (pin = OCMe₂CMe₂O), developed by Masuda et al.,⁷ is a useful synthetic route to aryl boronates. While initial mechanistic proposals included the deprotonation of HBpin by Et₃N, we have shown that this is not possible due to the hydridic nature of the B–H bond. Through our theoretical study, we established that the mechanism (Scheme 3) involves the expected oxidative addition of ArX to Pd(0). In contrast to Masuda's preliminary proposal, subsequent Et₃N-assisted ionization of the resulting L₂Pd(Ar)(X) complex generates the coordinatively unsaturated, 14-electron [L₂PdAr]⁺ cation, which reacts, via σ -bond metathesis, with HBpin to generate the ArBpin product and [L₂PdH]⁺; the latter is deprotonated by Et₃N to regenerate the L₂Pd(0) catalyst. Thus, the base Et₃N plays two roles, assisting the ionization process as well as reducing the Pd(II)-hydrido cation to Pd(0) via deprotonation. A similar catalytic cycle operates in the related Pd-catalyzed borylation of ArX using R₂NBH₂, developed by Alcaraz et al.¹¹

Acknowledgment. This work was supported by the Research Grants Council of Hong Kong (HKUST 602108 and 601507). T.B.M. thanks the Royal Society (UK) for support via an International Outgoing Short Visit Grant, the Royal Society of Chemistry for a Journals Grant for International Authors, and the EPSRC for support via an Overseas Research Travel Grant.

Supporting Information Available: Complete ref 19 and tables giving Cartesian coordinates and electronic energies for all of the calculated structures. This material is available free of charge via the Internet at <http://pubs.acs.org>.

(37) Amatore, C.; Jutand, A. *Acc. Chem. Res.* **2000**, *33*, 314.

(38) Alcaraz, G. Private communication.